Polarization measurements of Na $3p\ ^2P_{3/2}$ in Na-Ar, Na-Kr, and Na-Xe optical collisions

D. A. Olsgaard, M. D. Havey, and A. Sieradzan*
Department of Physics, Old Dominion University, Norfolk, Virginia 23529
(Received 26 December 1990)

Measurements of polarization of the Na $3p\ ^2P_{3/2}$ level produced in Na-Ar, Na-Kr, and Na-Xe optical collisions are reported. The measurements extend over a range of detunings from 150 cm^{-1} red to 350 cm^{-1} blue of resonant excitation of the Na $3p$ levels. The short-pulse, pump-probe technique employed in the experiments eliminates large systematic effects due to the hyperfine interaction, collisions, and radiative trapping. For far-blue-wing excitation, nearly constant polarizations of 21(2)%, 13(2)%, and 8(2)% are obtained for Na-Ar, Na-Kr, and Na-Xe, respectively.

I. INTRODUCTION

Collisional relaxation in isolated and in nearly degenerate excited states has been studied for many years.[1,2] In those studies, a multipole or distribution of multipoles is often produced by optical pumping, and the relaxation to lower-order multipoles is determined. As reflected in the normally large cross sections of several 100 $Å^2$, the relaxation rates are governed mainly by long-range interactions. Angular momenta of up to $200\hbar$ or more contribute significantly to the cross sections in many cases. Application of the optical-collision technique to the excitation of atomic multipoles[3] during a simultaneous radiative and collisional interaction has provided new insight into the physics of atomic multipole relaxation. In an optical collision, nonresonant light is absorbed during a collision between two atoms. After the collision, one or both of the atoms may be left in excited states. In addition to the excited populations produced, absorption of polarized light, even in an isotropic collision environment, may result in an atomic orientation[4] or alignment[5-12] after the optical collision is completed.

Depending on the frequency of the light, absorption during a collision may occur at small internuclear separations where specific molecular states or mixtures of states may be excited.[13] As the detuning Δ of the frequency of the light from resonance excitation is varied, both the range of contributing angular momenta ($<70\hbar$) and the final-state collision energy are also varied. These give the investigator an additional variable through which to study relaxation of atomic multipoles.

When one of the atomic products has several closely spaced levels, such as in a fine-structure multiplet, inelastic processes can also be studied through optical collisions.[14,15] In this case, branching fractions into the various accessible final states as Δ is varied are determined.[11,12,14,15] The interplay between these fractions and the atomic polarization as a function of the detuning provide a varied set of data through which insight into the various dynamic processes occurring during the optical collision may be obtained.

Earlier work has concentrated on atomic alignment produced in optical collisions involving rare-gas atoms and group II atoms in their lowest $^1P_1$ state.[3-8,16] Significant insights into how the atomic alignment depends on the details of the optical-collision dynamics have been obtained. For systems having significant spin interactions, more limited theoretical[17-20] and experimental[9-12] results on the alignment produced in optical collisions have been reported. Detailed experimental[14,15] and theoretical[18,21-25] results have been obtained on the inelastic fine-structure branching in Na–rare-gas optical collisions.

In this paper we report the results of extensive experiments on the polarization of the atomic Na $3p\ ^2P_{3/2}$ level produced in optical collisions with rare-gas atoms. The results are obtained through a pulsed, pump-probe technique which eliminates systematic effects in the data due to hyperfine interactions, subsequent collisions, or radiative trapping. Contrasting the results with those from group II–rare-gas-atom experiments allows the role of the spin-orbit interaction to be clarified. Comparison of the experimental data with available quantum-mechanical close-coupling calculations of the dynamics is also made.[12,18]

II. EXPERIMENT

The experimental technique is illustrated in Fig. 1, where illustrative relativistic potentials of a Na—rare-gas (RG) system[26] are shown as a function of internuclear separation. Linearly polarized light (frequency ν) from laser 1 (pump) is tuned into the far wings of the Na $3p\ ^2P_j$ doublet, where the detuning Δ is positive with respect to $D2$ for the blue wing $[\nu-\nu(D2)>0]$ and negative with respect to $D1$ for the red wing $[\nu-\nu(D1)<0]$. According to the classical Franck-Condon principle, radiative transitions for a detuning Δ will occur at internuclear separations R such that $V_X(R)+h\nu=V_B(R)+h\nu(D2)$. This relates the detuning to the difference potential by $\Delta=[V_B(R)-V_X(R)]/h$. It can be seen from Fig. 1 that far-blue-wing detunings correspond primarily to free-free molecular transitions between the $B\ ^2\Sigma_{1/2}$ and $X\ ^2\Sigma_{1/2}$ states; far-red-wing detunings correspond to free-free or free-bound molecular transitions between the $A\ ^2\Pi_{1/2,3/2}$ and $X\ ^2\Sigma_{1/2}$ states. After excitation the molecule dissociates on molecular terms that approach each other closely at large R. In that region rotational and spin-orbit in-

teractions may dominate the mixing of the molecular states.[24] As these states asymptotically correlate to the $3p\,^2P_{1/2}$ and $3p\,^2P_{3/2}$ atomic states, the result can be nonequilibrium populations in the $3p\,^2P_{1/2,3/2}$ levels and in the magnetic substrates of the $3p\,^2P_{3/2}$ level. The former effect has been previously investigated;[14,15] in this paper we have investigated the latter by observing the resulting alignment (polarization) in the $3p\,^2P_{3/2}$ state following the optical collision as a function of detuning.

The alignment $\langle A_0 \rangle$ is defined[27] as

$$\langle A_0 \rangle = \frac{\sum_M \{[3M^2 - J(J+1)]\sigma(J,M)\}}{\sum_M J(J+1)\sigma(J,M)} , \quad (1)$$

where J and M are the angular-momentum and z-axis projection quantum numbers. $\sigma(J,M)$ is the cross section for production of the state defined by J and M. Excitation of the colliding Na-RG pair with linearly polarized light produces a molecular alignment, a portion of which, in the average over all collisions, survives to produce a residual atomic alignment $\langle A_0 \rangle$. This is a measure of the axial symmetry of the Na $3p\,^2P_{3.2}$ electronic charge distribution produced, where the axis of symmetry is the linear polarization direction of the exciting light.

The alignment produced in the $3p\,^2P_{3/2}$ level is measured by probing with laser 2 (probe); the frequency of the laser is fixed to the $3p\,^2P_{3/2} \rightarrow 5s\,^2S_{1/2}$ resonance transition. Its linear polarization direction is periodically switched from parallel to perpendicular to laser 1, thus probing the polarization of the $^2P_{3/2}$ level populated in the optical collision.

Na atoms that are promoted to the $5s\,^2S_{1/2}$ state are detected via cascade fluorescence from the $4p\,^2P_j$ level at 330 nm. The resulting signal intensities $I_\parallel$ and $I_\perp$, corresponding to the two probe polarizations, determine the linear polarization given by $P_L = (I_\parallel - I_\perp)/(I_\parallel + I_\perp)$. The polarization is related to the alignment $\langle A_0(\Delta) \rangle$ by[27]

$$P_L = 3h\langle A_0(\Delta)\rangle / [4 + h\langle A_0(\Delta)\rangle], \quad (2)$$

where h is a geometrical factor equal to $-\frac{5}{4}$ for a $^2P_{3/2}$-$^2S_{1/2}$ transition. This expression is identical to that obtained for P_L in the case of observation of the $3p\,^2P_{3/2} \rightarrow 3s\,^2S_{1/2}$ fluorescence in the usual 90° geometry. Note that for resonant excitation of the $3p\,^2P_{3/2}$ level with linearly polarized light Eq. (1) gives $\langle A_0(D2) \rangle = -0.8$, which predicts a polarization of 60% in the absence of any depolarizing effects.

A schematic diagram of the experimental apparatus appears in Fig. 2. A short pulse (0.8 ns), 1-MW nitrogen laser simultaneously pumps dye lasers 1 and 2. At a repetition rate of 4 to 5 Hz, no stirring of the dye was required. The dye lasers are of the grazing incidence type where a 100% end mirror is used and the output coupling is the zeroth-order reflection from the grating. This arrangement provides for maximum laser power at the expense of a relatively large broadband background. The high power is especially important for the pump laser since the collision-induced absorption in the far wings is many orders of magnitude smaller than on resonance. The pump laser has an average pulse energy of about 18 μJ and a bandwidth of less than about 2 cm^{-1}. The probe laser has a typical pulse energy of about 14 μJ per pulse and a bandwidth of about 1 cm^{-1}. Both lasers are collimated to a beam size of less than 2 mm by a single lens at the output of each laser.

The pump laser is spectrally purified by a Na absorption-cell–prism combination. The absorption cell is approximately 35 cm long and contains Na and approximately 300 Torr RG. The heated filter cell removes,

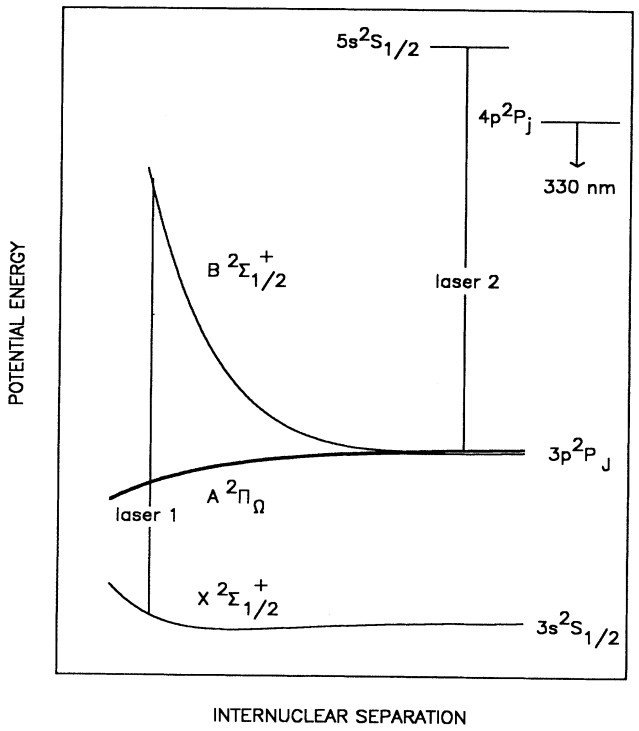

FIG. 1. Qualitative potentials for a Na–rare-gas molecule, illustrating the basic experimental scheme.

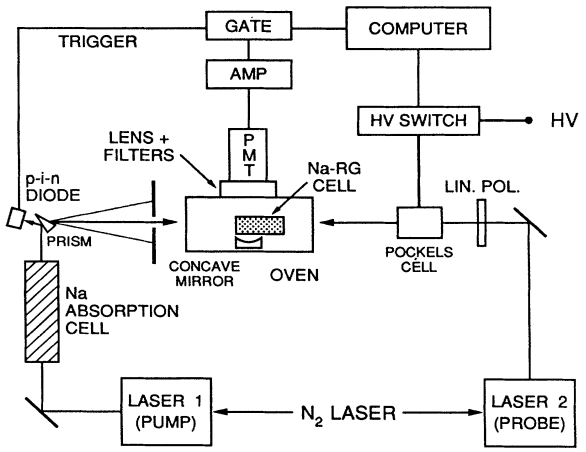

FIG. 2. A schematic diagram of the experimental apparatus.

from the broadband background of the laser, light resonant with the Na D lines. A rutile prism follows the absorption cell and strongly disperses the remaining broadband background upon which are superimposed a bright laser spot and dark "Fraunhöfer" lines at the $D1$ and $D2$ lines due to absorption by the filter cell. An iris at the entrance to the oven permits only the tuned laser beam to enter. For each detuning a slight rotation of the prism is thus required.

The linear polaroid and Pockels cell in the probe-laser path produce a probe polarization parallel or perpendicular to the horizontally polarized pump laser, as determined by a computer-controlled application of a half-wave voltage to the Pockels cell. The pump and probe laser beams enter the oven colinearly but from opposite sides.

The oven contained a sealed Na–RG cell and was heated by a coaxial heater; the temperature was stabilized to within about 0.1 K. Windows at each end of the oven allowed the laser beams to enter the oven and a side window at 90° permitted viewing of the fluorescence signal at the pump laser end of the cell. The sealed Na-RG cells were made of Pyrex tubing 6 to 7 cm long and 2.5 cm in diameter; the windows were perpendicular to the direction of the incoming laser beams. They were processed in a vacuum–gas-handling system by evacuation to less than 10^{-6} Torr and baking for typically 48 h at 650 K. A macroscopic amount of Na from a break seal ampoule was then flamed into each cell followed by the admission of a research grade RG (Ar, Kr, Xe) at the desired pressure (typically 2–20 Torr) as measured by a calibrated capacitance manometer. For this experiment, data were taken at a nominal temperature of 453 K, corresponding to a Na density of about 10^{12} cm^{-3}.

The $4p$-$3s$ fluorescence signal at 330 nm was gathered by a concave mirror, lens, and filter combination. The filter combination consisted of a 330-nm interference filter and 1 mm of Schott UG-11 colored glass which removed all background due to laser scattering and Na $D1$ and $D2$ resonance fluorescence . The detector was a cooled EMI 9814 bialkali-cathode, quartz-window photomultiplier tube (PMT) operated in a gated photon-detection mode. Photons were counted in a 500-ns gate which opened about 30 ns after the laser fired. The 30-ns delay eliminated the initial laser scattering pulse from the gate as well as high-frequency noise which appeared at the PMT output due to the firing of the N_2 laser. The noise otherwise appeared in the electronics as photon counts early in the gate. The counting rate was limited to about one photon count in ten laser shots in order to minimize dead time. Small dead-time corrections were made as necessary. However, for the far wings a counting rate of 0.1 photon per shot was typically all the signal available.

The experiment and data acquisition were computer controlled with a provision for the selection of the total number of laser shots and the polarization switching frequency. Switching the probe polarization frequently (typically every five laser shots) eliminated systematic effects due to drifting in the average laser characteristics in which one polarization orientation would have a higher average power than the other. The primary sources of these drifts were bleaching of the laser dyes after several hours of running, and a thermal drift in the effective probe-laser frequency due to longitudinal modes under the gain profile drifting in and out of resonance with the $3p\ ^2P_{3/2} \rightarrow 5s\ ^2S_{1/2}$ transition. Photon-counting data were accumulated and displayed for each polarization in real time. A time distribution of the accumulated photon counts, which was found useful for diagnostic purposes, was also obtained.

III. THE SHORT-PULSE PUMP-PROBE TECHNIQUE AND SYSTEMATIC EFFECTS

The measurements reported in this paper were made using a short-pulse pump-probe technique. This technique eliminates or greatly reduces several systematic effects that generally decrease the size of the measured polarization. The reduction of systematic effects in each case is due to the short time ($T < 0.5$ ns) the excited Na atoms produced in the optical collision are probed by laser 2.

First, the 16.3-ns radiative lifetime[28] of the $3p$ state is much longer than the probe width T. This has the effect of minimizing depolarization due to radiative trapping, for fewer than 3% of the excited atoms radiatively decay during the time the probe laser is on. This was confirmed experimentally by varying the signal size by a factor of 4, over which there was no measurable change in the wing polarization. As the signal size in the optical collision is linearly proportional to the Na density, this corresponded to a $\times 4$ change in that quantity.

A temperature dependence of the $D2$ resonance line polarization of about 20% could be observed, when the density was varied over an order of magnitude, depending on whether the fluorescence was viewed on the probe or pump side of the fluorescence cell (see Fig. 1). When the fluorescence was viewed on the pump side the effect was minimal. We believe the effect to be due to hole burning in the pump-laser spectral profile as it transverses the optically thick cell. When the signal is taken from the probe end, the pump laser propagates through the full length of the cell. Depending on the rare-gas pressure, the contribution to the measured polarization from the wings relative to resonant excitation is greatly enhanced in that case. Fluorescence signals were normally viewed from the pump side of the cell.

Second, depolarization due to unobserved hyperfine structure[29] can essentially be eliminated if the laser pulses are temporally much shorter than $\omega_{FF'}^{-1}$, where $\omega_{FF'}$ is the frequency splitting between hyperfine levels of angular momentum F and F'. Since the $I = \frac{3}{2}$ nuclear spin of Na couples with the electronic angular momentum $J = \frac{3}{2}$ to form $F = I + J$, J is no longer a constant of the motion. This introduces an oscillating time dependence in all the multipole moments of the electronic state represented by J. The time dependence of the multipole moment[29,30] corresponding to the alignment is given by

$$\langle A_0(\Delta,t)\rangle = g^{(2)}(t)\langle A_0(\Delta,0)\rangle ,$$
$$g^{(2)}(t) = \sum[(2F+1)(2F'+1)/(2I+1)] \times W^2(JFJF';I2)\cos\omega_{FF'}t . \quad (3)$$

Here, $W(\,)$ is a Racah coefficient and $\langle A_0(\Delta,0)\rangle$ is the electronic alignment at the moment of excitation. The sum is over the allowed values of F and F'. Note that at $t=0$, $g^{(2)}(0)=1$ and the alignment is just that produced in the electron charge cloud at the time of excitation. As t becomes greater than zero, J and I precess about F and the factor $g^{(2)}(t)$ decreases from its maximum value of 1. Since the time scales involved in an optical collision are short compared to a precession time, $t_{\rm coll}\sim 1$ ps $\ll\omega_{FF'}^{-1}$, the alignment following the optical collision is essentially $\langle A_0(\Delta,0)\rangle$. Consequently, using an overlapping short-pulse pump and probe as described above, we can freeze out the electronic alignment at $t=0$, or even at a later time $t>0$, by delaying the arrival time of the probe pulse.

We have computationally investigated the effectiveness of the pulsed pump-probe technique for the $3p\ ^2P_{3/2}$ level of Na. Equations (2) and (3) were used to compute $g^{(2)}$ and the resulting polarization is calculated as a function of pulse length and pump-probe delay, assuming square pulses for the pump and probe. For overlapping 0.5-ns pulses we calculate a polarization of 59.9%. If the probe is delayed by 2 ns, the polarization is already reduced to 50%, and by 8 ns the polarization reaches a minimum of -16%. By continuing to increase the probe delay, several oscillations of "polarization quantum beats" are mapped out. Experimentally we have checked these calculations by measuring the polarization for a 0- and 8-ns probe delay. We get 59% (2) and -15% (3), respectively. Calculations also show that longer pulses can be effectively shortened for $t=0$ measurements by advancing the probe arrival time relative to the pump; the remaining temporal overlap of the pulses will then be the effective pulse length.

For a continuous excitation Eq. (3) must be integrated[29] with a damping factor $e^{-t/\tau}$, where τ is the lifetime of the state, to get an average $g^{(2)}$. The result for the Na $3p\ ^2P_{3/2}$ level is 0.297, corresponding to a resonance polarization of 21%. Data taken with cw excitation must therefore be corrected by about a factor of 3 in order to account for the depolarizing influence of the hyperfine interaction.

Third, the short-pulse method can reduce depolarization due to collisions subsequent to the optical collision, so long as the rate Γ of depolarizing collisions[1] is such that $\Gamma T \ll 1$. For the wing excitation experiments reported here, there was no discernible pressure dependence to the measured polarization for $P<20$ Torr. For example, for Na-Kr at detunings of 50 and 250 cm^{-1}, the polarization did not change within the statistical uncertainty for variations of the pressure from 5 to 35 Torr. In all cases, the reported measurements were taken at pressures of 10 Torr or less, on the conservative side of this range.

Under the conditions that prevailed for the wing measurements, with rare-gas pressures in the 7–10-Torr range and cell temperature of 453 K, the resonance line polarization was $P_L=55(3)\%$. However, measurements of the $D2$ resonance-line polarization showed a clear decrease for pressures above 10 Torr, and for Na-Kr at 35 Torr the polarization was 40(5)%, well below the low-pressure limiting value of 60%. A decrease of this amount is approximately what one would expect, based on a rate-equation analysis of the depolarization using existing data for depolarization[1] and fine-structure changing[31] cross sections. The data suggest that there may be an anomalous, and as yet unexplained, reduction in the collisional depolarization rate for those excited atoms produced in a far-wing optical collision. A similar anomalously small relaxation rate has been previously measured[15] in optical-collision experiments on fine-structure branching in Na-Ar, Na-Kr, and Na-Xe.

Finally, we have made additional checks of our basic experimental technique, including the accuracy of the polarization switching of the probe laser. These are partly based on polarization measurements under conditions of pumping and probing of the $3p\ ^2P_{1/2}$ and $3p\ ^2P_{3/2}$ levels. For the former, we expect $P_L=0\%$, for a $J=\frac{1}{2}$ level cannot be aligned. We measure $P_L=0(2)\%$ for this case. For the latter, we measure $P_L=59(2)\%$ at $T=433$ K in a Na cell with no rare gas. In the absence of hyperfine depolarization, the expected polarization of the $J=\frac{3}{2}$ level is 60%. These checks confirm the overall absence, in our apparatus and technique, of a variety of possible systematic effects, including beam misalignment, imperfect polarization switching, and cell-window birefringence. In addition, the wing signal size was linear with variations in the pump-laser intensity over a factor of 3. On the other hand, the probe transition was readily saturated, although it was not strongly so under the usual operating conditions. Nevertheless, the polarization measurements reported here were independent of either the pump- or probe-laser intensity, even when the probe transition was saturated. A similar effect has been observed and explained for the case of a pump-probe optical-collision experiment in Ba-Ar.[4]

In conclusion, the wing polarization measurements reported here are, within their statistical uncertainty, independent of the depolarizing influences of radiation trapping, subsequent collisions, and the hyperfine interaction. They also did not depend in any measurable way on the intensity of either the pump- or the probe-laser intensity. Thus the results quoted in the following section are free from evident systematic error, within the quoted statistical uncertainties.

IV. RESULTS AND DISCUSSION

Polarization data for the red and blue wings of Na-Ar, Na-Kr, and Na-Xe are presented in Figs. 3–5. The data extend over a range of detunings from 150 cm^{-1} red to 350 cm^{-1} blue of the D lines. The range was limited by a rapidly decreasing signal size caused by a combination of decreasing laser power and absorption coefficient with increasing Δ. In addition, for red-wing excitation, as $-\Delta$ approaches kT, excitation is increasingly into bound states[32] of the $A\ ^2\Pi_\Omega$ wells; absorption that leads to excited Na $3p$ atoms then drops off more rapidly than the total

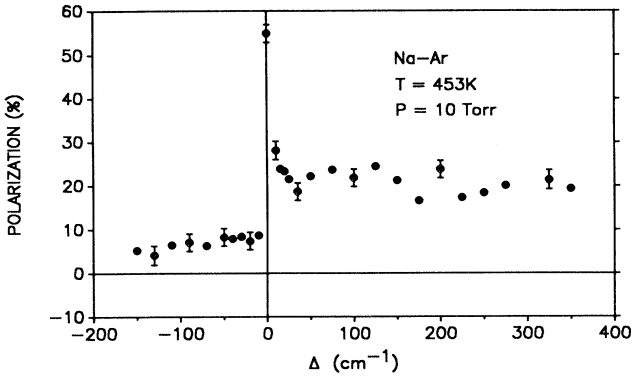

FIG. 3. Atomic Na $3p\ ^2P_{3/2}$ polarization as a function of detuning produced in Na-Ar optical collisions.

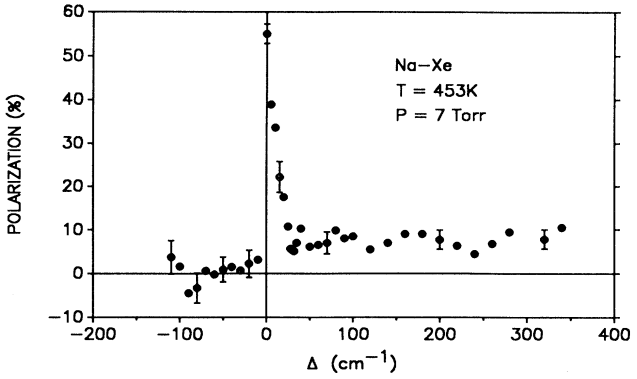

FIG. 5. Atomic Na $3p\ ^2P_{3/2}$ polarization as a function of detuning produced in Na-Xe optical collisions. The data for negative detunings were obtained with $P=2$ Torr and $T=443$ K.

absorption rate itself. The overall signal strength over the range of the data varied by about a factor of 100. The maximum signal size occurs in the near red wings of Na-Kr and Na-Xe, where strong absorption satellites[33,34] enhance the total signal. For $\Delta>0$, the signals do not drop off as fast as the overall absorption; this is because an increasing fraction of the Na $3p$ atoms branch into the $J=\frac{3}{2}$ level.[15]

The gap in the data at around $\Delta=300$ cm^{-1} is due to the presence of the $3s$-$4d$ two-photon resonance with the pump laser at 578.9 nm. This signal created a background larger than the wing excitation signal. This resonance did, however, serve as a convenient additional calibration point for the detuning of the pump laser, which has an overall accuracy of about ±1 cm^{-1}.

Data were taken in runs of 5000 shots with a background check every other run. The background counts were typically less than 5% of the total signal, and were subtracted from the measured $I_{\parallel}$ and $I_{\perp}$ before P_L was calculated. With a photon-counting rate of one in ten laser shots, typically 30 000 laser shots determined a point on the graph with a standard deviation of about $\pm2\%$. The error bars on the polarization data represent one standard deviation of error due to photon-counting statistics.

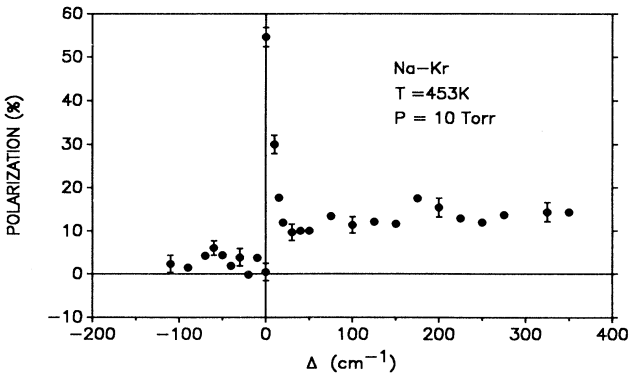

FIG. 4. Atomic Na $3p\ ^2P_{3/2}$ polarization as a function of detuning produced in Na-Kr optical collisions.

Of the data presented here, a comparison with other theoretical or experimental results is available only for Na-Ar (Fig. 3). For that case, our data are in overall agreement with the measurements of Ermers, Woschnik, and Behmenburg;[12] our results are several times more accurate, however, and more extensive. The measurements reported in Fig. 3 for Na-Ar are also in excellent agreement with the close-coupling calculations of Julienne and Vahala[18] and of Rebentrost.[35]

The results displayed in Figs. 3–5 show a generally positive polarization for both $\Delta>0$ and $\Delta<0$, with the polarization being larger for each collision pair in the blue wing. For $\Delta>0$, the polarization is seen to decrease from a value near 60% in the vicinity of $\Delta=0$ to a possible shallow minimum in the 30–35-cm^{-1} range. For larger detunings the polarization is nearly constant. When $\Delta<0$, the polarization is small for all three sets of data, and appears to decrease monotonically out to -150 cm^{-1}. The polarization is seen to increase in both the red and blue wings as the rare gas is changed from Xe to Kr to Ar. Note that a continuation of this trend is seen in the Na-He measurements of Ermers, Woschnik, and Behmenburg.[12] To our knowledge, no polarization measurements or calculations are available for Na-Ne.

An extension of the ideas[16] used to qualitatively understand the group II–rare-gas polarization results[3–8] can, by accounting for the spin-orbit interaction, provide a unified picture of the Na–RG polarization data. A main concept is that of an orbital locking radius R_L, within which a molecular electronic orbital follows the internuclear axis. For internuclear separations $R>R_L$, the orbital becomes space fixed. In an optical collision with $|\Delta|\gg0$, excitation takes place normally within a range of internuclear separations smaller than R_L. The optically excited orbital then remains molecule-fixed throughout the collision trajectory until $R>R_L$. For excitation of a molecular Σ state, the orbital lies in the collision plane. When a Π state is excited there are two possibilities; for one molecular parity the orbital lies in the collision plane,

while for the other it is perpendicular to the collision plane. A second important point is that the amount of rotation of an orbital is normally smaller for repulsive trajectories than for attractive ones. A smaller angle of rotation leads to a larger residual atomic polarization after an optical collision. These concepts form the qualitative basis for the Lewis-Cooper model,[16] which has had good success in quantitatively describing the results of the group II–RG-atom polarization experiments.

To apply these ideas to the Na–RG polarization data presented here, the added complications of the spin-orbit interaction must be accounted for. That this is necessary is evident from a comparison of the data for the group II–RG and Na–RG experiments; in the former case the far-red-wing polarization is significantly higher than that produced in far-blue-wing excitation. The reverse is true for the Na–rare-gas pairs, even though states of the same orbital symmetry (Σ for $\Delta \gg 0$ and Π for $\Delta \ll 0$) are excited in each case.

First consider far-blue-wing detunings, corresponding to excitation of the $B\,^2\Sigma^+_{1/2}$ molecular state. For this state, the spin is not space quantized along the internuclear axis; it is nominally described by Hund's case (b).[36] The spin is thus expected to play a lesser role in determining the dynamics of the molecular orbital. A similar point concerning blue-wing excitation has been made previously by Schuller, Nienhuis, and Behmenburg.[17] Further, although the orbital lies in the collision plane, the trajectories associated with the highly repulsive B state potential imply a relatively small orbital rotation between the point of excitation and R_L. Thus a significant residual polarization is expected for $\Delta \gg 0$. Decoupling of the spin from the orbital dynamics (so far as the residual atomic polarization is concerned) is clearly seen in the quantum-mechanical, close-coupling calculations of Julienne and Vahala[18] and Julienne,[37] for Na-Ar and for Na-He. Two sets of calculations are made, with one treating the electron spin as a spectator of the dynamics. The other set treats the spin as a full participant in the dynamics. Polarization results for $\Delta \gg 0$ are nearly the same in each case. Thus, far-blue-wing polarization produced in optical collisions from Na–RG and group II–RG pairs should be similar in magnitude; comparison of the data shows this to be the case.

In the red wings, when $-\Delta \gg 0$, optical excitation corresponds to production of Π molecular orbitals. In Hund's case (a) (Ref. 36) these are labeled $^2\Pi_{3/2}$ and $^2\Pi_{1/2}$; the two electronic states are split by the spin-orbit coupling constant A. Described in this basis the Π orbitals have a complex spatial representation and the spin and space parts of the wave function do not factor. They thus do not lend themselves to the physical picture so useful in understanding the group II–RG results. However, by representing the spin and angular parts of the case (a) wave function in terms of atomic-type orbitals, it is possible to construct linear combinations of case (a) states that factor into a real spatial part and a spinor. For each molecular parity these consist of a pair of orbitals, one in the collision plane and one perpendicular to it. In this basis, the spin-orbit coupling is completely off diagonal; the in-plane and out-of-plane orbitals are thus mixed dynamically by the spin-orbit interaction. For Na, when $A = 11.5\ \mathrm{cm}^{-1}$, this means that an out-of-plane orbital excited during an optical collision is rotated into the collision plane in about 1.4 ps. In fact, due to the near degeneracy[38] of the $^2\Pi_{1/2}$ and $^2\Pi_{3/2}$ states in Na–RG molecules there are nearly equal excitation amplitudes into each state; optical excitation then produces either an in-plane or out-of-plane orbital, depending on the relative phase of the excitation amplitude.

To apply this idea to the red-wing data, consider first collisions of duration much shorter than 1.4 ps. Then the optically excited orbitals either follow the internuclear axis out to $R = R_L$ (for the in-plane orbital) or remain fixed in space for all R (for the out-of-plane orbital). Thus the red-wing polarization is high for this case, in spite of the attractive trajectories, because the out-of-plane orbital is not rotationally depolarized. This situation should apply quite well to Na-He optical collisions, for a typical collision time is about 0.2 ps in that case. The measurements of Ermers, Woschnik, and Behmenburg[12] do indeed show a high polarization for Na-He.

For the heavier rare gases, the average collision time is longer (> 1 ps) and the out-of-plane orbital is brought, by the spin-orbit interaction, into the collision plane, where it is subsequently reoriented by molecular rotation. Thus the residual polarization in the red wings should become increasingly small as the rare gas is varied from Ar to Kr to Xe. This effect, in combination with the greater average deflection of the molecular orbitals for $-\Delta > 0$ excitation, accounts for the small red-wing residual polarization seen in Figs. 3–5. The main difference between the group II–RG and Na–RG results is then a much smaller red-wing residual polarization in the latter case. This results from a molecular fine-structure coherence in combination with the depolarizing influence of molecular rotation. This effect, along with the more attractive collision trajectories for red-wing compared to blue-wing excitation, accounts for the considerably smaller polarization measured when $\Delta \ll 0$.

V. CONCLUSIONS

The residual polarization in the $3p\,^2P_{3/2}$ level of Na, following optical collisions with Ar, Kr, and Xe, has been measured as a function of detuning from resonant excitation. The polarization measured in the blue wing is larger than that produced by red-wing excitation, but otherwise varies weakly with detuning. This is in contrast with the fine-structure branching,[15] which shows strong variation with detuning. We conclude that different mechanisms are important for determining the polarization and the fine-structure branching.

By introducing a basis of real spatial orbitals for the molecular Π states, an elaboration of the qualitative ideas behind the Lewis-Cooper model to include the spin-orbit interaction has been made. This description has made clear the important role of the spin-orbit interaction in determining the red-wing polarization. In contrast, the

spin-orbit interaction has little effect on the residual polarization following blue-wing excitation. The variation of the wing polarization with detuning and with rare gas for Na–RG optical collisions has been qualitatively described in a uniform way.

ACKNOWLEDGMENTS

We acknowledge fruitful discussions with P. Julienne and L. Vahala. The support for this research by the National Science Foundation is greatly appreciated.

*Permanent address: Department of Physics, Central Michigan University, Mt. Pleasant, MI 48859.

[1]W. E. Baylis, in *Progress in Atomic Spectroscopy,* edited by W. Hanle and H. Kleinpoppen (Plenum, New York, 1979).
[2]Alain Omont, Prog. Quantum Electron **5**, 69 (1977).
[3]K. Burnett, Phys. Rep. **118**, 339 (1985).
[4]W. J. Alford, N. Anderson, M. Belsley, J. Cooper, D. M. Warrington, and K. Burnett, Phys. Rev. A **31**, 3012 (1985).
[5]P. Thomann, K. Burnett, and J. Cooper, Phys. Rev. Lett. **45**, 1325 (1980).
[6]W. J. Alford, K. Burnett, and J. Cooper, Phys. Rev. A **27**, 1310 (1983).
[7]W. J. Alford, N. Anderson, K. Burnett, and J. Cooper, Phys. Rev. A **30**, 2366 (1984).
[8]M. Belsley and J. Cooper, Phys. Rev. A **35**, 1013 (1987).
[9]W. Behmenburg and V. Kroop, J. Phys. B **14**, 427 (1981).
[10]W. Behmenburg, V. Kroop, and F. Rebentrost, J. Phys. B **18**, 2693 (1985).
[11]W. Behmenburg, Phys. Scr. **36**, 300 (1987).
[12]A. Ermers, T. Woschnik, and W. Behmenburg, Z. Phys. D **5**, 113 (1987).
[13]A. Gallagher, Acta. Phys. Pol. A **54**, 721 (1978).
[14]M. D. Havey, G. E. Copeland, and W. J. Wang, Phys. Rev. Lett. **50**, 1767 (1983).
[15]M. D. Havey, F. T. Delahanty, L. L. Vahala, and G. E. Copeland, Phys. Rev. A **34**, 2758 (1986).
[16]E. L. Lewis, M. Harris, W. J. Alford, J. Cooper, and K. Burnett, J. Phys. B **16**, 553 (1983).
[17]F. Schuller, G. Nienhuis, and W. Behmenburg, Z. Phys. D **2**, 193 (1986).
[18]P. S. Julienne and L. L. Vahala, in *Spectral Line Shapes,* edited by R. Exton (Deepak, Hampton, 1987), Vol. 4.
[19]F. Rebentrost, R. Best, and W. Behmenburg, J. Phys. B **20**, 2627 (1987).
[20]A. Ermers, W. Behmenburg, and F. Schuller, Z. Phys. D **10**, 437 (1988).
[21]K. C. Kulander and F. Rebentrost, Phys. Rev. Lett. **51**, 1262 (1983).
[22]K. C. Kulander and F. Rebentrost, J. Chem. Phys. **80**, 5626 (1984).
[23]F. Rebentrost, J. Phys. B **19**, L121 (1986).
[24]L. L. Vahala, P. S. Julienne, and M. D. Havey, Phys. Rev. A **34**, 1856 (1986).
[25]R. Best and F. Rebentrost, J. Phys. B **20**, 4087 (1987).
[26]E. Czuchaj and J. Sienkiewicz, Z. Naturforsch. A **34**, 694 (1979).
[27]C. H. Greene and R. N. Zare, Annu. Rev. Phys. Chem. **33**, 119 (1982).
[28]B. P. Kibble, G. Copley, and L. Krause, Phys. Rev. **153**, 9 (1967).
[29]K. Blum, *Density Matrix Theory and Applications* (Plenum, New York, 1981).
[30]U. Fano and J. H. Macek, Rev. Mod. Phys. **45**, 53 (1973).
[31]J. Apt, and D. Pritchard, J. Phys. B **12**, 83 (1979).
[32]M. Belsley, W. J. Alford, K. Burnett, and J. Cooper, J. Quant. Spectrosc. Radiat. Transfer **35**, 53 (1986).
[33]W. P. West and A. Gallagher, Phys. Rev. A **17**, 1431 (1978).
[34]M. J. Jongerius, T. Hollander, and C. Th. Alkemade, J. Quant. Spectrosc. Radiat. Transfer **26**, 285 (1981).
[35]As given in Ref. 12.
[36]G. Herzberg, *Spectra of Diatomic Molecules,* 2nd ed. (Van Nostrand Reinhold, New York, 1950).
[37]P. S. Julienne (private communication).
[38]For example, see E. Zanger, V. Schmatloch, and D. Zimmermann, J. Chem. Phys. **8**, 5396 (1988).